Enhanced Enantioselectivity in Excitation of Chiral Molecules by Superchiral Light

Yiqiao Tang, *et al.*

Science **332**, 333 (2011);
DOI: 10.1126/science.1202817

5. S. Lloyd, S. L. Braunstein, *Phys. Rev. Lett.* **82**, 1784 (1999).
6. M. Dakna, T. Anhut, T. Opatrny, L. Knöll, D.-G. Welsch, *Phys. Rev. A* **55**, 3184 (1997).
7. A. P. Lund, T. C. Ralph, H. L. Haselgrove, *Phys. Rev. Lett.* **100**, 030503 (2008).
8. A. Ourjoumtsev, R. Tualle-Brouri, J. Laurat, P. Grangier, *Science* **312**, 83 (2006).
9. J. S. Neergaard-Nielsen, B. M. Nielsen, C. Hettich, K. Mølmer, E. S. Polzik, *Phys. Rev. Lett.* **97**, 083604 (2006).
10. K. Wakui, H. Takahashi, A. Furusawa, M. Sasaki, *Opt. Exp.* **15**, 3568 (2007).
11. A. Ourjoumtsev, H. Jeong, R. Tualle-Brouri, P. Grangier, *Nature* **448**, 784 (2007).
12. See supporting material on *Science* Online.
13. H. Jeong, A. P. Lund, T. C. Ralph, *Phys. Rev. A* **72**, 013801 (2005).
14. M. Hillery, R. F. O'Connell, M. O. Scully, E. P. Wigner, *Phys. Rep.* **106**, 121 (1984).
15. D. T. Smithey, M. Beck, M. G. Raymer, A. Faridani, *Phys. Rev. A* **70**, 1244 (1993).
16. A. I. Lvovsky, *J. Opt. B* **54**, S556 (2004).
17. S. L. Braunstein, H. J. Kimble, *Phys. Rev. Lett.* **80**, 869 (1998).
18. B. Schumacher, *Phys. Rev. A* **54**, 2614 (1996).
19. M. Ban, *Phys. Rev. A* **69**, 054304 (2004).
20. F. Grosshans, P. Grangier, *Phys. Rev. A* **64**, 010301(R) (2001).
21. L. Mišta Jr., R. Filip, A. Furusawa, *Phys. Rev. A* **82**, 012322 (2010).
22. H. Takahashi *et al.*, *Phys. Rev. Lett.* **101**, 233605 (2008).
23. J. S. Neergaard-Nielsen *et al.*, *Phys. Rev. Lett.* **105**, 053602 (2010).
24. D. Gottesman, A. Kitaev, J. Preskill, *Phys. Rev. A* **64**, 012310 (2001).

25. Supported by the Strategic Information and Communications R&D Promotion (SCOPE) program of the Ministry of Internal Affairs and Communications of Japan, Special Coordination Funds for Promoting Science and Technology, Grants-in-Aid for Scientific Research, Global Center of Excellence, Advanced Photon Science Alliance, and Funding Program for World-Leading Innovative R&D on Science and Technology (FIRST) commissioned by the Ministry of Education, Culture, Sports, Science and Technology of Japan, Academy of Sciences of the Czech Republic, Japanese Society for the Promotion of Science, and the Australian Research Council, Center of Excellence (grant CE11E0096).

Supporting Online Material

www.sciencemag.org/cgi/content/full/332/6027/330/DC1
Materials and Methods

30 November 2010; accepted 14 February 2011
10.1126/science.1201034

Enhanced Enantioselectivity in Excitation of Chiral Molecules by Superchiral Light

Yiqiao Tang[1] and Adam E. Cohen[1,2]*

A molecule or larger body is chiral if it cannot be superimposed on its mirror image (enantiomer). Electromagnetic fields may be chiral, too, with circularly polarized light (CPL) as the paradigmatic example. A recently introduced measure of the local degree of chiral dissymmetry in electromagnetic fields suggested the existence of optical modes more selective than circularly polarized plane waves in preferentially exciting single enantiomers in certain regions of space. By probing induced fluorescence intensity, we demonstrated experimentally an 11-fold enhancement over CPL in discrimination of the enantiomers of a biperylene derivative by precisely sculpted electromagnetic fields. This result, which agrees to within 15% with theoretical predictions, establishes that optical chirality is a fundamental and tunable property of light, with possible applications ranging from plasmonic sensors to absolute asymmetric synthesis.

Circular dichroism (CD) describes the differential absorption of left- and right-circularly polarized light by a chiral molecule (*1*). CD spectroscopy provides important structural information and is widely used for characterizing organic and biological molecules. Yet CD measurements are challenging because the signals are typically weak. For most small molecules, the absorption cross sections for left- and right-circularly polarized light differ by less than one part per thousand (*2*).

The weakness of CD is a consequence of the small size of most molecules relative to the wavelength of light: The circularly polarized field undergoes a barely perceptible twist over a distance of molecular dimensions (*3*). This twist provides only a weak perturbation to the overall rate of excitation. Finding ways to enhance CD could lead to improved sensors and may open the door to efficient absolute asymmetric synthesis in which light provides the chiral bias.

[1]Department of Physics, Harvard University, 12 Oxford Street, Cambridge, MA 02138, USA. [2]Department of Chemistry and Chemical Biology, Harvard University, 12 Oxford Street, Cambridge, MA 02138, USA.

*To whom correspondence should be addressed. E-mail: cohen@chemistry.harvard.edu

Substantial effort has been devoted to calculating CD spectra for a variety of molecules at multiple levels of theory (*4*, *5*) and to designing molecules that show large optical dissymmetry at particular wavelengths (*2*). These treatments focused on the molecular aspects of CD, relying on circularly polarized plane waves as the source of excitation.

With the advent of near-field optics, plasmonics, photonic crystals, and metamaterials, scientists now construct electromagnetic fields that are far more contorted than is circularly polarized light (CPL) (*6*, *7*). Several groups have sought to use metallic nanostructures to enhance chiroptical phenomena (*8*–*10*). Recently, Hendry *et al.* reported enhanced CD in samples of proteins adsorbed onto chiral metal nanostructures (*11*). These experiments may lead to important practical applications, but the complexity of the geometries has thus far prevented a quantitative comparison with theory. Other groups have applied techniques of coherent control to enantioselective excitation of chiral molecules, but these strategies are specific to a single compound or narrow class of compounds (*12*).

We wondered whether it would be possible to design non–plane-wave monochromatic solutions to Maxwell's equations that showed enhanced dissymmetry in their excitation of all chiral molecules, regardless of molecular structure. Our intuitive picture was that enhanced dissymmetry should occur if the field lines reoriented over a distance much shorter than the free-space wavelength, ideally over molecular dimensions. Then the spatial scales of chirality in the molecule and the light would match (*13*).

To guide the design of superchiral light, we sought a measure of optical chirality, a way to determine whether one field couples more strongly to molecular chirality than does another (*14*). Such a measure must have certain symmetries. Chirality is time even (a movie of a right-handed screw shows a right-handed screw whether the movie is played forward or backward), parity odd (a mirror image of a right-handed screw is a left-handed screw), and scalar (a right-handed screw remains right-handed no matter its orientation). A classification of the well-known conserved electrodynamic quantities by their symmetries (Fig. 1A) reveals a vacancy where there should be a time-even, parity-odd scalar. Any measure of optical chirality must lie in this empty fourth quadrant (*15*).

On the basis of these symmetry considerations, we proposed the existence of a physical quantity, optical chirality, defined in Fig. 1A. The mathematical structure of optical chirality captures the degree to which the electric and magnetic field vectors **E** and **B** wrap around a helical axis at each point in space. In the 1960s, Lipkin studied this same quantity, but he and others dismissed it as lacking physical significance (*16*, *17*).

Is optical chirality observable? In the standard theory of CD, the dissymmetry factor, $g(\lambda)$, measures the fractional difference in rates of excitation between left- and right-circularly polarized light at wavelength λ (*18*). We generalized the theory of CD to include pairs of arbitrary mirror-image fields and found that the dissymmetry factor becomes (*14*)

$$g = g_{\mathrm{CPL}}\left(\frac{cC}{2U_e\omega}\right) \qquad (1)$$

where g_{CPL} is the dissymmetry factor under circularly polarized light, c is the speed of light,

C is the optical chirality, U_e is the local electric energy density, and ω is the angular frequency. The quantity g_{CPL} is purely molecular, a function of molecular transition moments and energy levels. The quantity $(cC/2\omega U_e)$ is purely electrodynamic. The fact that these two quantities combine in a simple product implies that, if one can enhance the ratio $(cC/2\omega U_e)$ relative to its value for CPL, then one can enhance the dissymmetry in light-matter interactions for all chiral molecules.

Equation 1 was derived for a model in which CD arises through an interference between electric dipole and magnetic dipole transitions. This model is valid in an isotropic sample, that is, one with a large number of molecules, all randomly oriented. The formula is equally valid for molecules that are freely tumbling, as in a liquid, or randomly immobilized, as in a polymer matrix. The possible contribution of electric dipole–electric quadrupole transitions in anisotropic samples is discussed below. Equation 1 does not apply to chiral structures of size comparable to the free-space wavelength, in which case higher multipole transitions contribute to CD.

In CPL, the field vectors rotate at a constant rate along the propagation direction, undergoing a complete revolution once per wavelength (Fig. 1B). In this case, the quantity $cC/2\omega U_e = 1$. Do Maxwell's equations permit solutions in which this quantity exceeds 1? We deduced the existence of superchiral light as follows. First, we drew a configuration of electric fields that appears highly chiral (Fig. 1C, bottom). The field vectors rotate through nearly 180° in a distance much shorter than half the free-space wavelength. Then we sought solutions to Maxwell's equations that generated these fields in at least one point in space. An optical standing wave was a promising candidate because near the nodes U_e is small, yet the field appears to have a strong twist. To achieve a chiral configuration, the standing wave is made from counterpropagating beams of CPL of opposite handedness and slightly different amplitude. The resulting superchiral field configuration is shown in Fig. 1C. Near the nodes of this standing wave, $g/g_{CPL} > 1$ (*14*).

Superchiral light is easily generated by reflecting CPL off a mirror with reflectivity $R < 1$: At normal incidence, the reflected wave has opposite handedness, slightly lower intensity, and a fixed phase relative to the incident wave—precisely the conditions needed to generate superchirality upon interference with the incident wave. If a chiral molecule is placed at a node in a superchiral wave, the dissymmetry is predicted to be enhanced by a factor of

$$g/g_{CPL} = (1 + \sqrt{R})/(1 - \sqrt{R}) \qquad (2)$$

which becomes large as R approaches 1.

We performed a conceptually simple experiment to probe the interaction of superchiral light with chiral matter. Several factors combined to dictate the choice of chiral molecule. The regions of enhanced chiral selectivity were too thin to detect by direct differential absorption, so we sought a fluorescent compound with which we could detect differential induced fluorescence (*19*). Many chiral molecules are fluorescent in the ultraviolet, but we sought a compound with visible excitation and emission because of the availability of better optics and more stable light sources in the visible. The molecule also needed to have a large value of g_{CPL} at a wavelength close to an available laser line. The chiral biperylene derivative shown in Fig. 2A met these requirements (*20*).

The key challenge was to position a 10-nm-thick film of the chiral compound relative to a mirror with a separation that drifted by less than $\lambda/10^4 \approx 0.5$ Å over the course of the experiment.

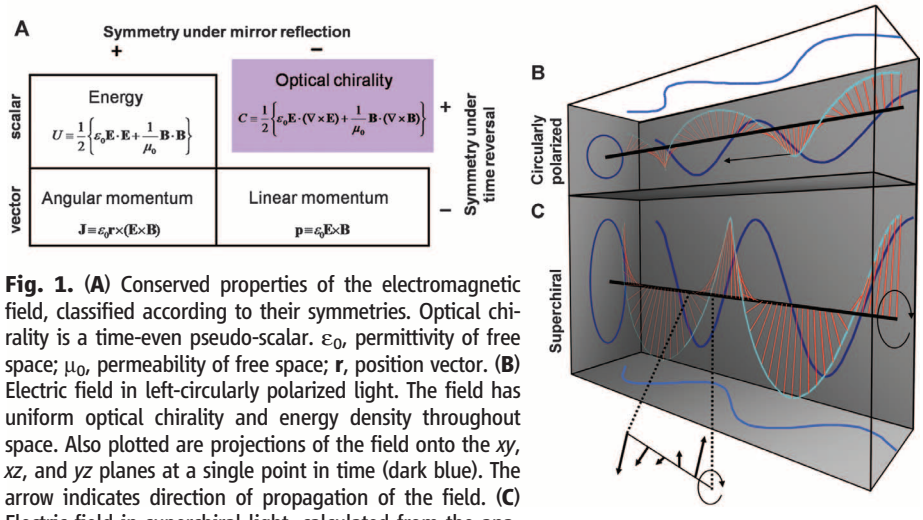

Fig. 1. (**A**) Conserved properties of the electromagnetic field, classified according to their symmetries. Optical chirality is a time-even pseudo-scalar. ε_0, permittivity of free space; μ_0, permeability of free space; **r**, position vector. (**B**) Electric field in left-circularly polarized light. The field has uniform optical chirality and energy density throughout space. Also plotted are projections of the field onto the *xy*, *xz*, and *yz* planes at a single point in time (dark blue). The arrow indicates direction of propagation of the field. (**C**) Electric field in superchiral light, calculated from the analytical expression at a single point in time. The superchiral field rotates about its axis but does not propagate. At any instant, the projection of the field along the propagation axis is an ellipse, but over time the field at each point traces out a circle. Near the superchiral nodes, the ratio of optical chirality to electric energy density is larger than in CPL. In this plot, the ratio of the left- and right-field amplitudes is 2:1. In the experiment, the ratio was 1.17:1. (Bottom) Field configuration near a superchiral node.

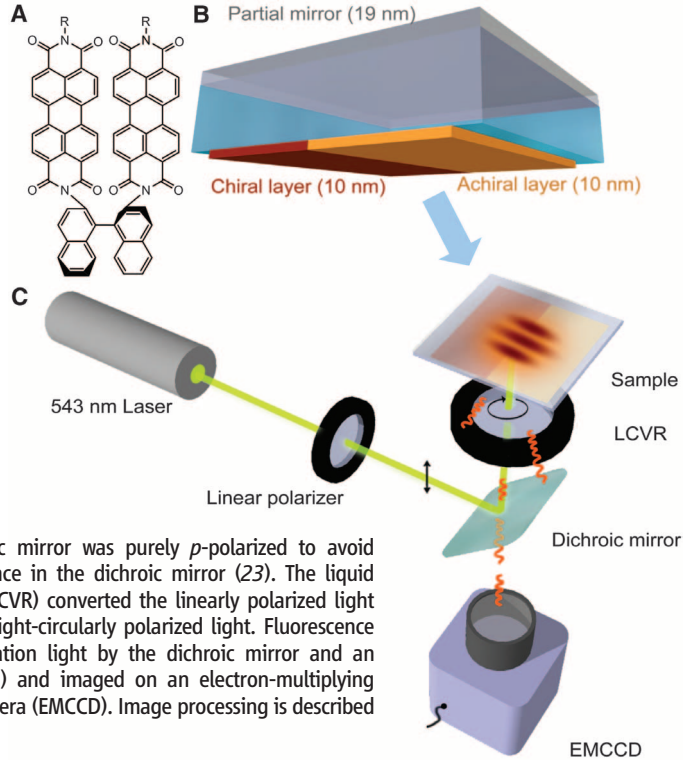

Fig. 2. (**A**) Chiral fluorophores consisted of the p (shown here) and m enantiomers of a binaphthylene-perylenebiscarboxydiimide dimer (*20*). R indicates 1-hexylheptyl group. (**B**) Nanofabricated structure for positioning a chiral fluorescent film with extreme stability relative to a partially reflecting mirror. The achiral fluorescent film served as a built-in control. The glass coverslip separating the chiral film from the mirror was 170 μm thick. (**C**) Apparatus for generating and detecting superchiral light. Light impinging on the dichroic mirror was purely *p*-polarized to avoid distortion from birefringence in the dichroic mirror (*23*). The liquid crystal variable retarder (LCVR) converted the linearly polarized light alternately into left- and right-circularly polarized light. Fluorescence was separated from excitation light by the dichroic mirror and an emission filter (not shown) and imaged on an electron-multiplying charge-coupled device camera (EMCCD). Image processing is described in detail in (*21*).

To achieve this stability, we fabricated the sandwich geometry shown in Fig. 2B (*21*). A 19-nm-thick Al mirror was deposited on one side of a glass coverslip, yielding a reflectivity $R = 0.72$. The other side of the coverslip was coated with a 10-nm-thick film of the chiral fluorophores in an amorphous polymer host. Half of the chiral film was then removed by plasma etching and replaced with an equivalent film of an achiral perylene derivative to serve as a control. We made two samples containing opposite enantiomers in the chiral region.

The samples were placed in an optical system designed to generate superchiral light (Fig. 2C). CPL ($\lambda = 543$ nm) was directed through the chiral film onto the mirror at normal incidence, with the expectation that the partially reflected wave would interfere with the incident wave to generate a standing wave with superchiral nodes. A slight wedge angle between the faces of the coverslip caused different regions of the chiral film to reside in different parts of the standing wave, with an in-plane fringe spacing of 2 mm. We took measures to compensate for pointing instability and power fluctuations in the laser, as well as all systematic artifacts, allowing fluorescence intensity measurements to a fractional precision of 4×10^{-5} (*21*). We imaged the fluorescence from the film alternately under left- and right-superchiral light and calculated a dissymmetry factor at each point in the image, based on the fractional difference in fluorescence under mirror-image field configurations.

Figure 3, top, shows plots of the average fluorescence intensity as a function of position in the superchiral standing wave, and Fig. 3, bottom, shows plots of the dissymmetry factor along a line cutting through a superchiral node. The superchiral nodes were located by their correspondence with a minimum in the average fluorescence intensity. The maximum dissymmetry factors were $g = 1.50 \times 10^{-2} \pm 0.08 \times 10^{-2}$ (SEM) and $g = -1.65 \times 10^{-2} \pm 0.08 \times 10^{-2}$ for the p and m enantiomers, respectively. The achiral control samples had $g \approx 0$ throughout the standing wave.

To determine the degree of superchiral enhancement, we repeated the experiments by using conventional CPL. Samples were prepared identically to above, except that the partially reflecting mirror was omitted so that no standing wave was generated. The dissymmetry factors under conventional CPL were $g_{CPL} = 1.41 \times 10^{-3} \pm 0.03 \times 10^{-3}$ (for p) and $g_{CPL} = -1.42 \times 10^{-3} \pm 0.04 \times 10^{-3}$ (for m) and were independent of position (fig. S4). Thus, the superchiral enhancements were 10.6 ± 0.6 (for the p enantiomer) and 11.6 ± 0.6 (for the m enantiomer).

A quantitative comparison of these results to theory requires consideration of the roles of several types of electronic transitions. Conventional CD in isotropic media (solid or liquid) arises through an electric dipole–magnetic dipole interference. This is the transition studied in (*14*) and described by Eq. 1. The present experiment involves molecules immobilized in an amorphous polymer host. Alhough we deem it unlikely, it is conceivable that the ensemble of fluorophores developed a net orientation through short-range interactions with the glass substrate during the deposition of the polymer film. In oriented chiral molecules, electric dipole–electric quadrupole transitions may contribute to CD as well.

We recently calculated the contribution of electric dipole–electric quadrupole transitions to optical dissymmetry in arbitrary electromagnetic fields (*22*). The relevant local field property is a third-rank tensor, $\Theta_{ijk} = E_i \frac{\partial}{\partial x_j} E_k$, where i, j, and k each vary over the three Cartesian coordinates. Remarkably, for the superchiral fields studied here, the enhancement in optical dissymmetry due to electric dipole–electric quadrupole transitions is identical to the enhancement due to electric dipole–magnetic dipole transitions (*22*). Thus, the fields are truly superchiral in that they do not distinguish between the two sources of molecular optical dissymmetry.

On the basis of these considerations, we find that the enhancement in optical dissymmetry is expected to be a function only of the reflectivity of the Al mirror, given by Eq. 2, regardless of possible orientational order in the film. For a film with reflectivity $R = 0.72$, Eq. 2 predicts a 12.2-fold enhancement at the superchiral nodes, within 15% of the experimental value.

The physical origin of this enhancement is somewhat subtle. A simple calculation shows that the optical chirality is the sum of the optical chiralities of the incident and reflected waves. This quantity is independent of position—it shows no special features at the nodes. Where, then, does the enhanced dissymmetry come from? The enhanced dissymmetry comes from the suppression of the electric energy density at the nodes. Pure electric dipole transitions form an achiral background and are excited at a rate proportional to the electric energy density. At the nodes, the achiral background becomes small, and so the fractional difference in excitation between mirror-image fields becomes large. This fact is illustrated in Fig. 3, bottom, where the black lines are proportional to the inverse of the average fluorescence intensity. The enhanced dissymmetry factor comes at the expense of a decreased overall rate of excitation.

It is perhaps surprising that superchiral light can be created with far-field optics alone. One might expect near-field or plasmonic effects to be necessary to generate highly twisted fields. This observation led us to ask whether there are any local configurations of electric and magnetic fields and field gradients that can be made with near-field but not far-field optics. One could imagine that the constraints imposed on propagating plane waves might rule out certain local field configurations that were otherwise allowed by Maxwell's equations. In (*22*), we showed that any local field configuration allowed by Maxwell's equations can be created at a single point in space through judicious interference of multiple far-field plane waves. These exotic local fields can enhance a wide variety of molecular multipole transitions, of which the chiral ones discussed here are but one example. Many of these

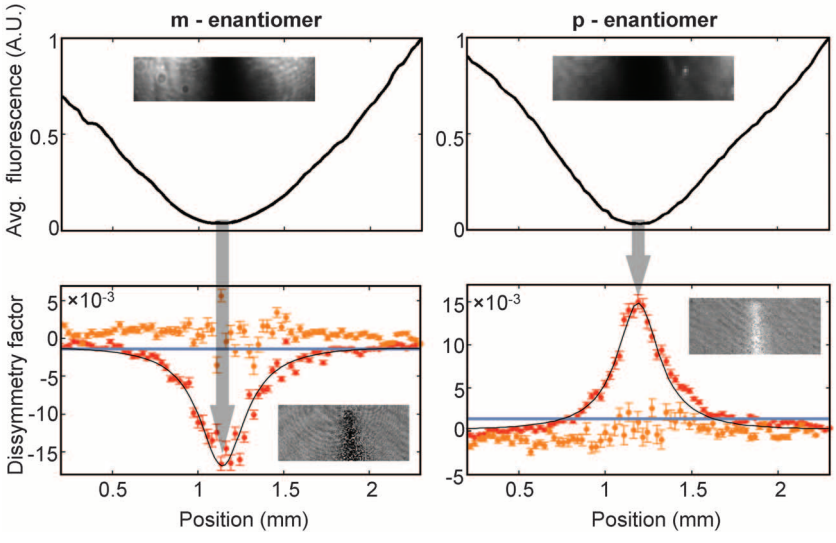

Fig. 3. Observation of enhanced optical dissymmetry in superchiral light. (**Top**) Average fluorescence intensity distribution in a superchiral standing wave. Superchiral nodes were identified by their correspondence with minima in the average fluorescence intensity. A.U., arbitrary units. (Insets) Images of the average fluorescence. (**Bottom**) Dissymmetry factor along a line cutting through a superchiral node in chiral (red) and achiral (orange) regions. Blue line marks the value of the position-independent dissymmetry factor measured in chiral films without superchiral enhancement. Black line is the theoretical prediction for the dissymmetry factor, calculated in (*21*). Error bars are SEM of 400 measurements. (Insets) Spatial maps of the dissymmetry factor near the superchiral nodes.

multipole spectroscopies have not previously been demonstrated.

The chiral enhancement reported here is not a fundamental limit. Larger enhancement may be obtained at the expense of lower overall excitation rate simply by choosing a mirror with a higher reflectivity. Enantioselective excitation with superchiral light can be performed on any chiral small molecule and requires only an inexpensive continuous-wave laser. The existence of superchiral light raises exciting possibilities to sculpt the three-dimensional shape of the electromagnetic field, to bring other dark transitions to light.

References and Notes

1. L. D. Barron, *Molecular Light Scattering and Optical Activity* (Cambridge Univ. Press, Cambridge, 2004).
2. N. Berova, K. Nakanishi, R. Woody, *Circular Dichroism: Principles and Applications* (Wiley, New York, 2000).
3. S. F. Mason, *Molecular Optical Activity and the Chiral Discriminations* (Cambridge Univ. Press, New York, 1982).
4. J. Autschbach, T. Ziegler, S. J. A. van Gisbergen, E. J. Baerends, *J. Chem. Phys.* **116**, 6930 (2002).
5. P. J. Stephens, *J. Phys. Chem.* **89**, 748 (1985).
6. E. Ozbay, *Science* **311**, 189 (2006).
7. M. Aeschlimann *et al.*, *Nature* **446**, 301 (2007).
8. I. Lieberman, G. Shemer, T. Fried, E. M. Kosower, G. Markovich, *Angew. Chem. Int. Ed.* **47**, 4855 (2008).
9. V. P. Drachev *et al.*, *J. Opt. Soc. Am. B* **18**, 1896 (2001).
10. V. A. Fedotov, A. S. Schwanecke, N. I. Zheludev, V. V. Khardikov, S. L. Prosvirnin, *Nano Lett.* **7**, 1996 (2007).
11. E. Hendry *et al.*, *Nat. Nanotechnol.* **5**, 783 (2010).
12. M. Shapiro, P. Brumer, *Rep. Prog. Phys.* **66**, 859 (2003).
13. N. Yang, Y. Tang, A. E. Cohen, *Nano Today* **4**, 269 (2009).
14. Y. Tang, A. E. Cohen, *Phys. Rev. Lett.* **104**, 163901 (2010).
15. L. D. Barron, *Nature* **238**, 17 (1972).
16. D. M. Lipkin, *J. Math. Phys.* **5**, 696 (1964).
17. T. W. B. Kibble, *J. Math. Phys.* **6**, 1022 (1965).
18. L. Rosenfeld, *Z. Phys. A Hadrons Nuclei* **52**, 161 (1929).
19. D. H. Turner, I. Tinoco Jr., M. Maestre, *J. Am. Chem. Soc.* **96**, 4340 (1974).
20. H. Langhals, J. Gold, *Liebigs Ann.* **1997**, 1151 (1997).
21. Materials and methods are detailed in supporting material available on *Science* Online.
22. N. Yang, A. E. Cohen, *J. Phys. Chem. B*, published online 6 January 2011 (10.1021/jp1092898).
23. Y. Tang, T. A. Cook, A. E. Cohen, *J. Phys. Chem. A* **113**, 6213 (2009).

Acknowledgments: We thank H. Langhals for the chiral biperylene compound and L. Men for help with the figures. Financial support was provided by the Nano-Enabled Technology Initiative of MITRE Corporation, a Defense Advanced Research Projects Agency Young Faculty Award, the Office of Naval Research Young Investigator Program, and the Harvard Center for Nanoscale Systems.

Supporting Online Material

www.sciencemag.org/cgi/content/full/332/6027/333/DC1
Materials and Methods
Figs. S1 to S4

13 January 2011; accepted 17 February 2011
10.1126/science.1202817

Deterministic Preparation of a Tunable Few-Fermion System

F. Serwane,[1,2,3]*† G. Zürn,[1,2]† T. Lompe,[1,2,3] T. B. Ottenstein,[1,2,3]‡ A. N. Wenz,[1,2] S. Jochim[1,2,3]

Systems consisting of few interacting fermions are the building blocks of matter, with atoms and nuclei being the most prominent examples. We have created a few-body quantum system with complete control over its quantum state using ultracold fermionic atoms in an optical dipole trap. Ground-state systems consisting of 1 to 10 particles are prepared with fidelities of ~90%. We can tune the interparticle interactions to arbitrary values using a Feshbach resonance and have observed the interaction-induced energy shift for a pair of repulsively interacting atoms. This work is expected to enable quantum simulation of strongly correlated few-body systems.

The exploration of naturally occurring few-body quantum systems such as atoms and nuclei has been extremely successful, largely because they could be prepared in well-defined quantum states. Because these systems have limited tunability, researchers created quantum dots—"artificial atoms"—in which properties such as particle number, interaction strength, and confining potential can be tuned (*1*, *2*). However, quantum dots are generally strongly coupled to their environment, which hindered the deterministic preparation of well-defined quantum states.

In contrast, ultracold gases provide tunable systems in a highly isolated environment (*3*, *4*). They have been proposed as a tool for quantum simulation (*5*, *6*), which has been realized experimentally for various many-body systems (*7*–*10*). Achieving quantum simulation of few-body systems is more challenging because it requires complete control over all degrees of freedom: the particle number, the internal and motional states of the particles, and the strength of the interparticle interactions. One possible approach to this goal is using a Mott insulator state of atoms in an optical lattice as a starting point. In this way, systems with up to four bosons per lattice site have been prepared in their ground state (*11*, *12*). Recently, single lattice sites have been addressed individually (*13*).

In single isolated trapping geometries, researchers could suppress atom number fluctuations by loading bosonic atoms into small-volume optical dipole traps (*14*–*18*). However, these experiments were not able to gain control over the system's quantum state.

We prepare few-body systems consisting of 1 to 10 fermionic atoms in a well-defined quantum state, making use of Pauli's principle, which states that each single-particle state cannot be occupied by more than one identical fermion. Therefore, the occupation probability of the lowest-energy states approaches unity for a degenerate Fermi gas, and we can control the number of particles by controlling the number of available single-particle states. We realize this by deforming the confining potential such that quantum states above a well-defined energy become unbound. This approach requires a highly degenerate Fermi gas in a trap whose depth can be controlled with a precision much higher than the separation of its energy levels.

To fulfill these requirements, we use a small-volume optical dipole trap with large level spacing. This microtrap is created by the focus of a single laser beam (Fig. 1) with a waist of $w_0 \lesssim 1.8$ μm and measured radial and axial trapping frequencies $(\omega_r,\omega_a) = 2\pi \times (14.0 \pm 0.1, 1.487 \pm 0.010)$ kHz (*19*). We load the microtrap from a reservoir of cold atoms. The reservoir consists of a two-component mixture of ^{6}Li atoms in the two lowest-energy Zeeman substates $|F = 1/2, m_F = +1/2\rangle$ and $|F = 1/2, m_F = -1/2\rangle$ (labeled state $|1\rangle$ and $|2\rangle$) in a large-volume optical dipole trap. The reservoir has a degeneracy of $T/T_F \approx 0.5$ (*19*), where T_F is the Fermi temperature. We superimpose the microtrap with the reservoir and transfer about 600 atoms into the microtrap. After removal of the reservoir, the degeneracy of the system is determined by $T_F \approx 3$ μK in the microtrap and the temperature $T \lesssim 250$ nK

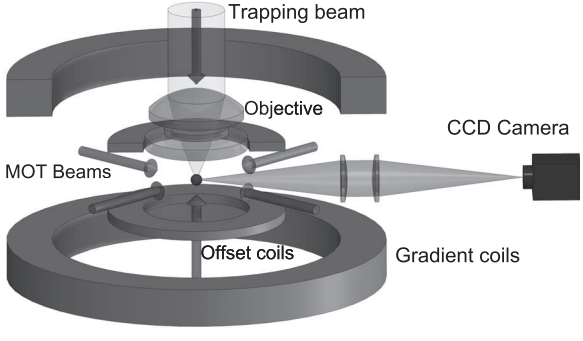

Fig. 1. Experimental setup. Systems with up to 10 fermions are prepared with ^{6}Li atoms in a micrometer-sized optical dipole trap created by the focus of a single laser beam. The number of atoms in the samples is detected with single-atom resolution by transferring them into a compressed magneto-optical-trap (MOT) and collecting their fluorescence on a CCD camera. A Feshbach resonance allows one to tune the interaction between the particles with a magnetic offset field.

[1]Physikalisches Institut, Ruprecht-Karls-Universität Heidelberg, 69120 Heidelberg, Germany. [2]Max-Planck-Institut für Kernphysik, Saupfercheckweg 1, 69117 Heidelberg, Germany. [3]ExtreMe Matter Institute EMMI, GSI Helmholtzzentrum für Schwerionenforschung, 64291 Darmstadt, Germany.

*To whom correspondence should be addressed. E-mail: friedhelm.serwane@mpi-hd.mpg.de
†These authors contributed equally to this work.
‡Present address: DIOPTIC GmbH, Bergstraße 92A, 69469 Weinheim, Germany.